JOURNAL OF MATERIALS SCIENCE 31 (1996) 3769–3775

Studies on fusion zone fracture behaviour of electron beam welds of an α + β-titanium alloy

T. MOHANDAS, D. BANERJEE, Y. R. MAHAJAN,
Defence Metallurgical Research Laboratory, Hyderabad, India
V. V. KUTUMBA RAO
Department of Metallurgical Engineering, Banaras Hindu University, Varanasi India

A study was undertaken to understand the fusion zone fracture behaviour of electron beam welded α + β-titanium alloy Ti–6.5 Al–3.3 Mo–1.8 Zr and 0.25 Si. The effect of base metal microstructure, the amount of heat input and post weld heat treatment cycle on the all-weld tensile properties and fracture behaviour was investigated in this work. In general, it was found that the tensile strength and ductility of α + β-base welds are higher than that of the β-base welds and the difference was attributed to the presence of wider fusion zone grains of β-base welds. The β-base weld tensile specimens always exhibited an intergranular fracture mode irrespective of the amount of heat input. The single pass low heat input α + β-base welds failed by ductile transgranular fracture mode, while high heat input single pass welds failed by a mixed mode (intergranular plus faceted) fracture. In general high heat input welds showed low ductility mainly on account of the strain localization effects at the grain boundary alpha phase. Post-weld heat treatments of α + β-base welds resulted in the improvement of tensile ductility and were associated with transgranular fracture due to the absence of strain localization effects at the grain boundary alpha phase.

1. Introduction

In the welding of titanium alloys, it is generally observed that the ductility of the weld fusion zone (FZ) is a function of fusion zone grain size [1]. The smaller the FZ grain size, the higher is the ductility. For this reason, low heat input welds, such as laser welds exhibit higher ductility, compared to high heat input gas tungsten arc welds. In earlier studies it was found that gas tungsten arc welds (GTAW) of the α + β-alloys Ti–6Al–6V–2Sn (Ti–662) and Ti–6Al–2Sn–4Zr–6Mo (Ti–6246) possess a large fusion-zone grain size [2–4]. Tensile fracture in the case of Ti–662 was reported to be transgranular, while in Ti–6246, which contained α″ phase, it was a mixed (transgranular + intergranular) type. Both these welds exhibited low macroscopic plastic deformation, although ductile microvoid coalescence features could be seen at high magnifications. Post-weld heat-treated (PWHT) Ti–662, GTAW samples containing Widmanstätten and grain boundary alpha phases were reported to exhibit transgranular fracture [5] while intergranular fracture was observed in the case of Ti–6246 [6]. An easy transfer of slip from grain boundary to the interior occurs in the case of Ti–662, but slip localization at grain boundaries takes place in Ti–6246 due to the large strength difference between the grain boundary and the grain interior which arises as a result of the higher molybdenum content in this alloy [6]. The above studies have been based mostly on tests conducted on composite tensile specimens, but little information is available in the literature on the all-weld tensile properties of α + β-alloy welds. The present study has been undertaken to elucidate the effect of base metal microstructure, amount of heat input and post-weld heat treatment in the substransus and supertransus regions on the all-weld tensile properties and fracture behaviour of an indigenously developed α + β-titanium alloy called GTM 900 (Ti–6.5Al–3.3Mo–1.8Zr–0.25Si). This alloy is intended for use in gas turbine disc applications. Electron beam welding (EBW) is the preferred method of fabrication for this application. Therefore EBW has been chosen for the present study. It is important to note here that all-weld tensile fracture characteristics of low heat input welds is hitherto unreported and hence this study assumes a special significance.

2. Experimental details

2.1. The material

The alloy used in this programme (GTM 900) was obtained from Mishra Dhathu Nigam Limited, Hyderabad, India, in the form of 110 mm square cross-section billet forged at 950 °C in the α + β-region. The chemical composition of the alloy is given in Table I.

0022–2461 © *1996 Chapman & Hall*

TABLE I Chemical composition of the parent alloy

Element	ppm								
	C	Al	Mo	Zr	Si	O	N	H	Ti
Wt %	0.013	6.8	3.42	1.9	0.21	920	65	54	Bal.

β-transus of the alloy is 1010 °C.

TABLE II Electron beam welding parameters

Base metal heat treatment	Speed of welding (cm min^{-1})	Number of passes (remelts)	Heat input (KJ cm^{-1})	Designation of the sample
α + β	260	2	1.94 × 2	αβ-260-2
	200	1	2.5	αβ-200-1
	120	1	4.2	αβ-120-1
β	260	2	1.94 × 2	β-260-2
	200	1	2.5	β-200-1

Beam voltage = 150 kV.
Beam current = 56 mA.

2.2. Electron beam welding

Electron beam welding was carried out on a Hawker-Siddley high voltage (150 kV) electron beam welding machine of 12 kW capacity at the Gas Turbine Research Establishment (GTRE), Bangalore, India.

The welding conditions used were a fixed beam voltage of 150 kV and beam current of 56 mA. Heat input was varied by changing the speed of welding and by remelting. Focus was adjusted to get full penetration up to 10 mm thickness, the thickness of the weld coupon at the joint. The parameters used are given in Table II.

2.3. Pre- and post-weld heat treatment

The as-received parent metal billet was cut into slices of 110 mm × 110 mm × 14 mm. The material was subjected to two types of heat treatment prior to welding. The heat treatments essentially consisted of two steps, namely, a solutionizing treatment either in the α + β- or β-range followed by a stabilization treatment at 530 °C. The β-treatment was carried out in a vacuum furnace at 1030 °C and the α + β-treatment was carried out at 960 °C in air in an electrical resistance heated muffle furnace. Stabilization treatments were carried out in a muffle furnace. The parent alloy heat treatment schedules are given Table III. Post-weld heat treatments were carried out either in the α + β- or β-regions. These treatments were similar to those used for the parent alloy. The oxide layer formed during the course of the heat treatments was removed by grinding. Details of the post-weld heat treatment are given in Table IV.

TABLE III Pre-weld heat treatment of the parent alloy

Designation of heat treatment	Details of heat treatment
α + β	960 °C/1 h/AC/530 °C/6 h/AC
β	1030 °C/15 min/FC (360 °C/h) /530 °C/8 h/AC

AC: air cooled; FC: furnace cooled.

TABLE IV Post-weld heat treatments

Base metal heat treatment	Post-weld heat treatment	Designation of the sample
	530 °C/6 h/AC	αβ-200-1
	960 °C/1 h/AC + 530 °C/6 h/AC	αβ-P960-1-AC
α + β	1030 °C/15 min/FC (360 °C/1 h) + 530 °C/6 h/AC	αβ-P1030-1/4-AC
β	530 °C/6 h/AC	β-200-1

Post-weld heat treatments were carried out only on weld coupons welded at a welding speed of 200 cm min^{-1}.

2.4. Specimen preparation and testing

Round tensile specimens were prepared from the butt joint weld coupons. Two types of specimen configurations, namely, a transverse tensile specimen with the weld located at the centre of the gauge and transverse to the loading axis and an all-weld tensile specimen. The specimen configurations used are given in Fig. 1. Standard metallographic specimen preparation procedures were adopted to study the microstructure using optical as well as scanning electron microscopes. Mechanical properties were determined on an Instron 1100 screw-driven machine. All mechanical properties were evaluated after a stabilization treatment at 530 °C. Fracture surface features were observed in ISI 100 and Jeol scanning electron microscopes.

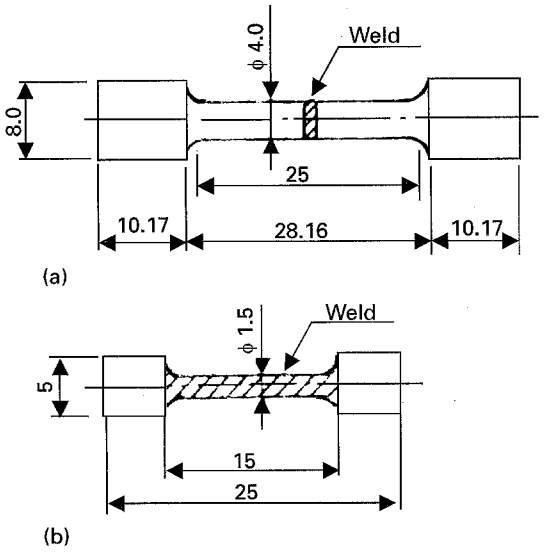

Figure 1 Tensile specimens: (a) transverse tensile and (b) all-weld tensile.

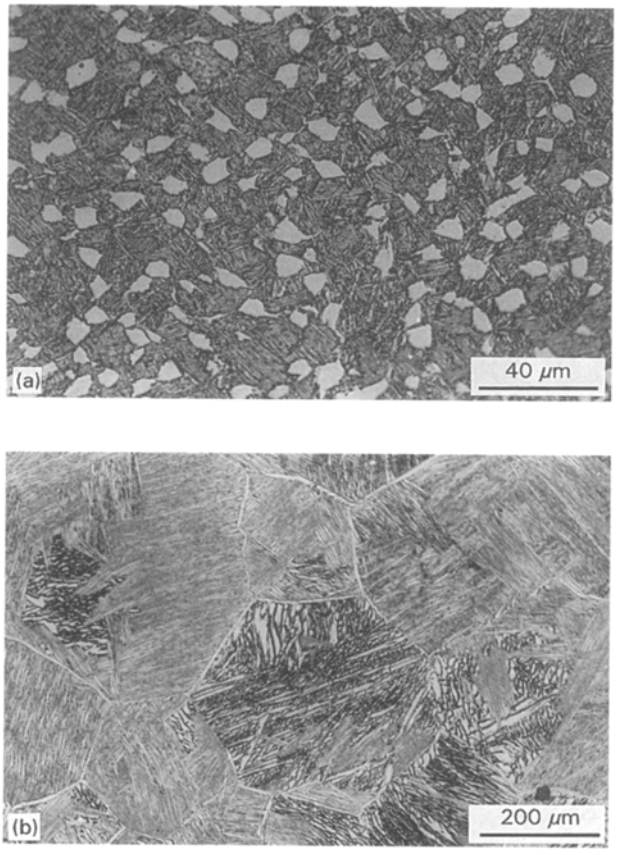

Figure 2 Base metal microstructure: (a) α + β heat treated and (b) beta heat treated.

3. Results

The microstructures of the parent material in the two heat-treated conditions are shown in Fig. 2. The fusion zone grain morphology and microstructures are presented in Fig. 3. Microstructures in the PWHT conditions are shown in Fig. 4. The ultimate tensile strength (UTS), the 0.2% yield strength (YS) and percentage elongation values obtained from the tensile tests are summarized in Table V.

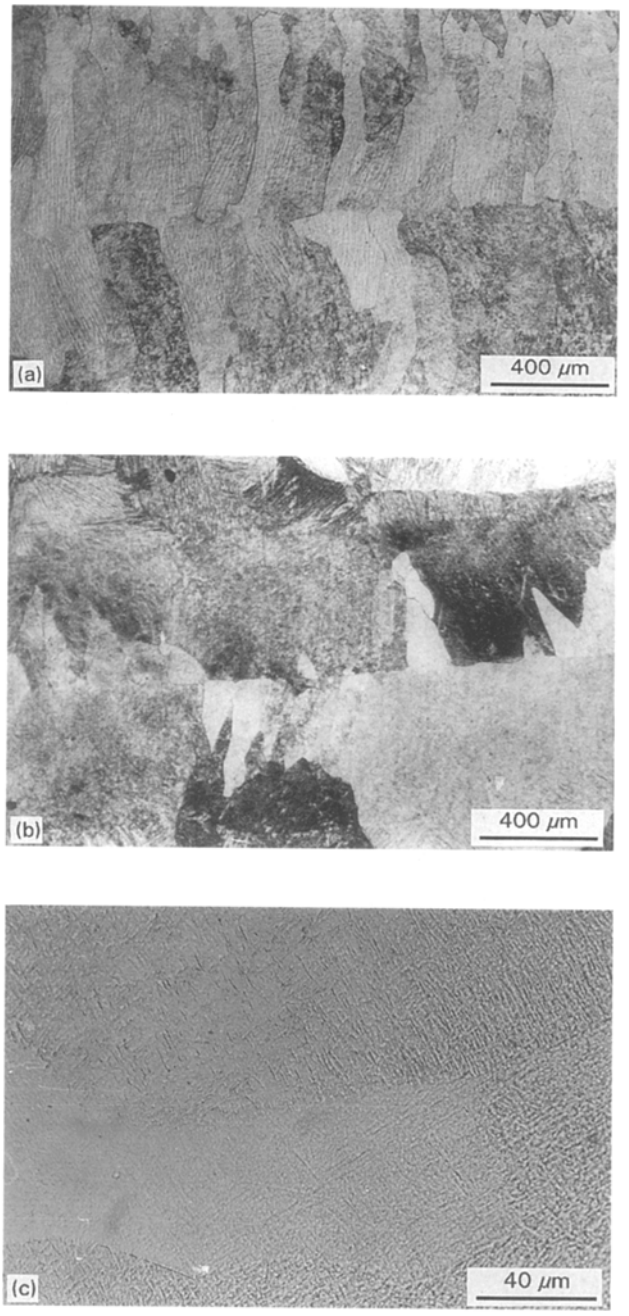

Figure 3 Weld zone macrostructure and microstructure: (a) α + β-base weld, (b) β-base weld and (c) general microstructure of fusion zone.

3.1. Metallography

The microstructure of the parent alloy in the α + β heat-treated condition consists of equiaxed primary α- and transformed β-phases (Fig. 2a). The β-treatment results in colonies of aligned α-laths with a thin layer of β-phase sandwiched between the α-laths. This structure also contains grain boundary alpha phase (Fig. 2b). The prior beta phase grain size in α + β-condition is 35–50 μm and in β-condition 350 μm. The width of the fusion zone grains in the β-base welds is greater compared to that in α + β-base welds (Fig. 3). The microstructure of the fusion zone consists of acicular α′ martensite (Fig. 3c). Post-weld heat treatment in the α + β-region resulted in coarsening of the transgranular α-phase microstructure due to the decomposition of α′ martensite into α + β-phase. Grain

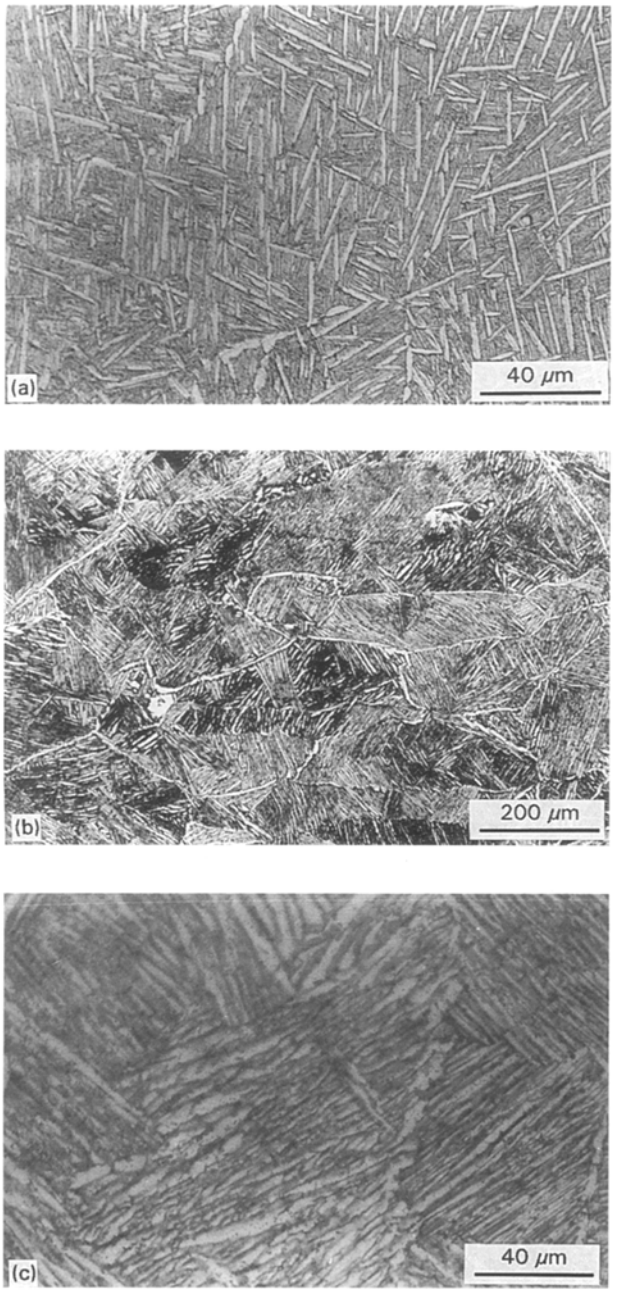

Figure 4 Microstructure in the post-weld heat-treated condition: (a) subtransus PWHT, (b) and (c) supertransus PWHT.

TABLE V Tensile properties of welds

Designation of the specimen	0.2% YS (MPa)	UTS (MPa)	Elongation (%)
αβ-120-1	1113	1213	3
αβ-200-1	1145	1392	4
αβ-260-2	1201	1401	3
αβ-P960-1-AC	1043	1136	7
αβ-P1030-1/4-FC[a]	860	927	8
αβ base metal	945	1010	18
β-200-1	1211	1334	3
β-260-2	1241	1332	2
β-base metal	873	942	11

[a] Transverse tensile.

boundary α-phase is discontinuous (Fig. 4a). Post-weld heat treatment in the β-region led to colony-type aligned transgranular α-phase with continuous grain boundary α-phase (Fig. 4b and c). The thickness of

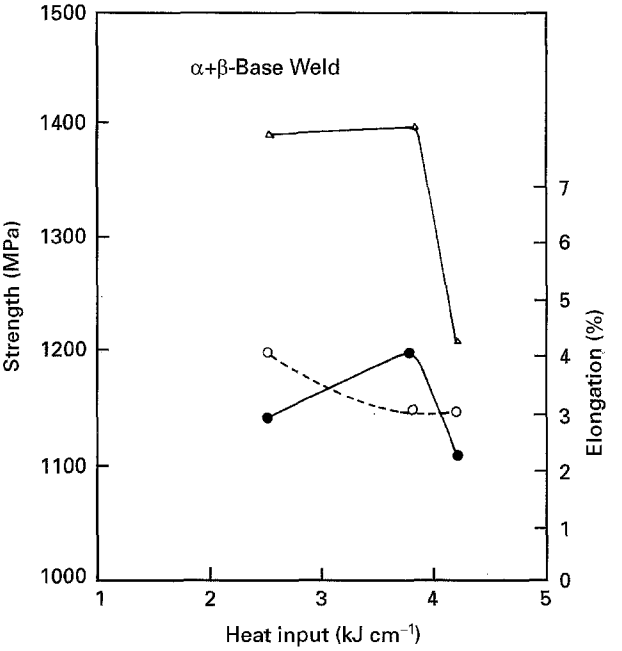

Figure 5 Effect of heat input on tensile properties. Note: intermediate heat input is by two-pass welding. Key: △ UTS; ● YS; ○ elongation %.

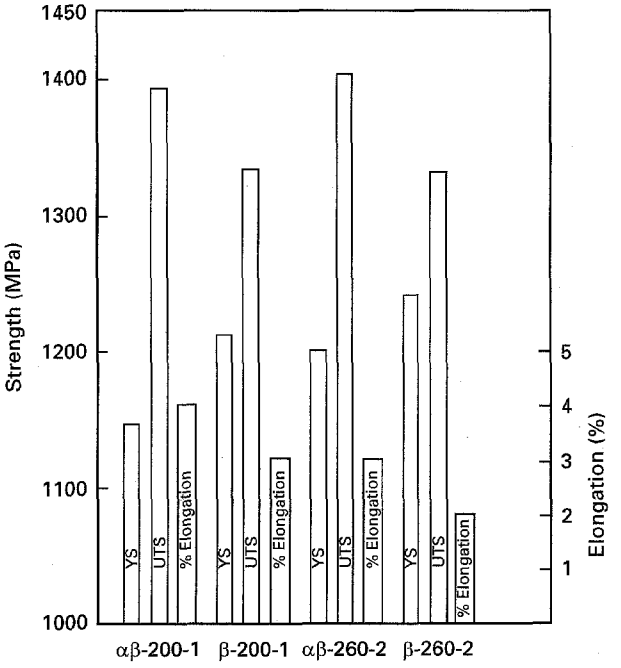

Figure 6 Effect of base metal microstructure on tensile properties of welds.

transgranular α-phase is larger in the case of the specimens subjected to supertransus post-weld heat treatment.

3.2. Tensile properties

The tensile properties are compared on the basis of heat input (Fig. 5), base metal microstructure (Fig. 6) and post weld heat treatment (Fig. 7). Fig. 5 shows that increased heat input has resulted in decreased strength and ductility; compare αβ – 200 – 1 with αβ – 120 – 1. However two pass welds at high speed

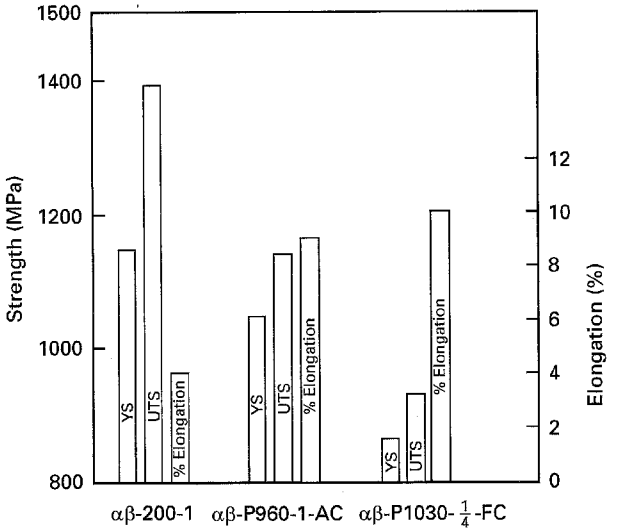

Figure 7 Effect of post-weld heat treatment on tensile properties.

led to reduced ductility only ($\alpha\beta - 260 - 2$). These observations on two pass welds are applicable in the case of β-base welds as well. From Fig. 6 it may be noted that the ultimate tensile strength and ductility of β-base welds are lower compared to α + β-base welds. In general the welds are of higher strength and lower ductility (Table V) compared to the base metal (Table V). The effect of PWHT is a reduction in strength and an improvement in ductility. Post-weld heat treatment in the β-region led to the lowest strength (Fig. 7).

3.3. Fractography

The fractographs of the tensile specimens of α + β-base welds are shown in Fig. 8, while those of β-welds are shown in Fig. 9. In Fig. 10 fractographs of PWHT specimens are presented. From Fig. 8 it is observed that single-pass low-heat input α + β-base welds failed by ductile transgranular fracture, while high heat input single-pass welds failed by a mixed mode of intergranular and faceted fracture. Two-pass welds exhibited faceted fracture. The β-base welds irrespective of heat input failed by intergranular fracture with martensite lath decohesion features at transgranular locations. In general both α + β- and β-base welds showed shallow ductile dimples. In the PWHT conditions ductile transgranular fracture was observed (Fig. 10). In the case of post-weld heat treatment in the β-region flutes were observed corresponding to the aligned alpha microstructure.

4. Discussion

The observed high strength and low ductility of welds is due to the presence of a martensitic microstructure. The high strength is associated with the fine nature of the martensite laths which is equivalent to a small grain size. The low ductility of the martensitic microstructure can be ascribed to low incubation strain for void nucleation [7] and fast void growth resulting in low fracture strain [8–11]. The high strength and low

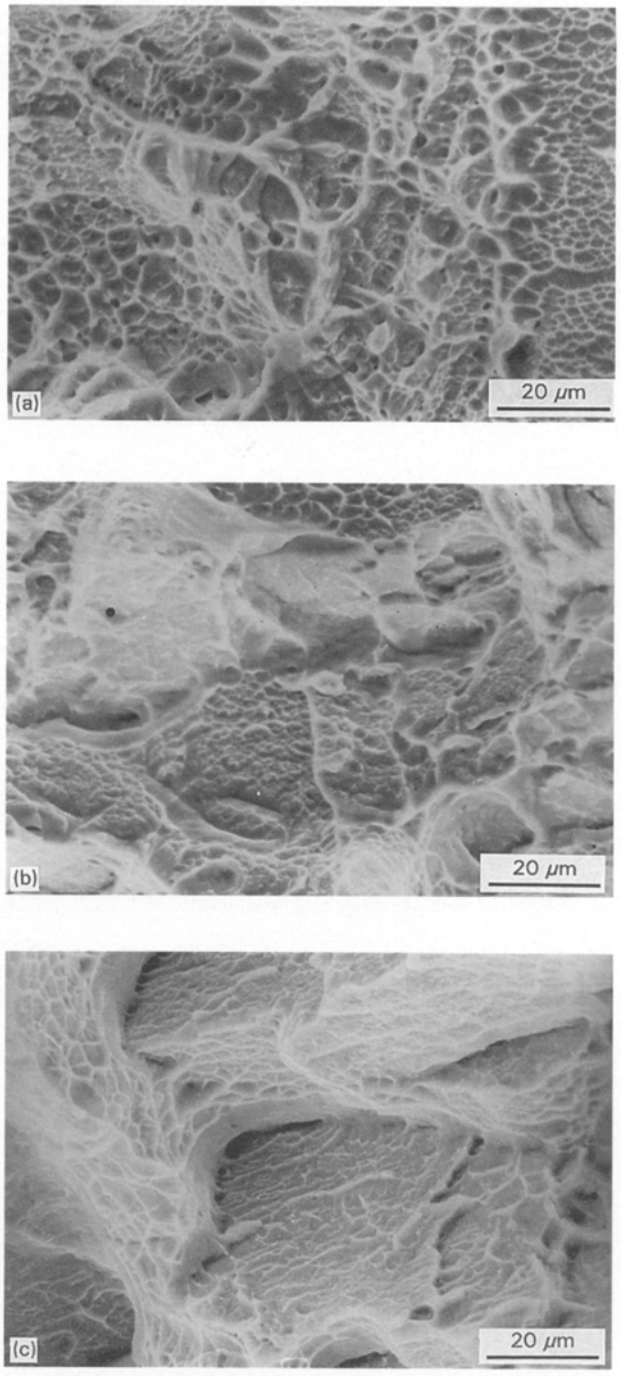

Figure 8 Fractographs of α + β-base welds: (a) αβ-200-1, (b) αβ-260-2 and (c) αβ-120-1.

ductility of the welds is in conformity with those observed in alloys with similar microstructures [1–4].

Reduction in strength and ductility in the high heat input single pass welds can be attributed to strain localization effects at the grain boundary due to the strength difference between a soft grain boundary and a strong grain interior [6, 10]. This effect would be more prominent at larger grain sizes [8]. Data on fusion zone grain widths support this view (Table VI). Further support is derived from the nature of the fracture which is both intergranular and faceted at large grain sizes but is essentially transgranular at lower grain sizes (Fig. 8). The observed faceted fracture in two-pass welds can be attributed to strain localization between primary and secondary martensite laths.

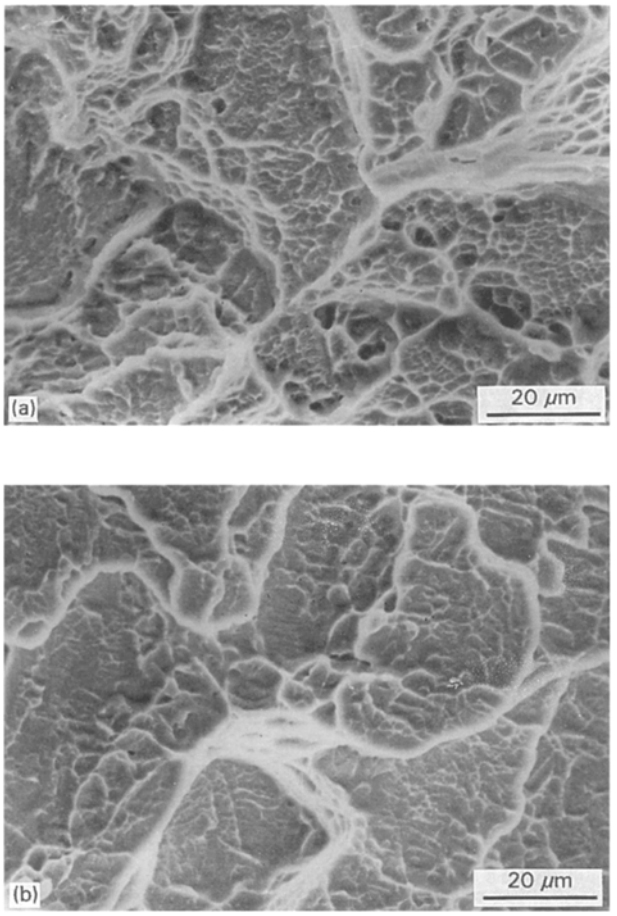

Figure 9 Fractographs of β-base welds: (a) β-200-1 and (b) β-260-2.

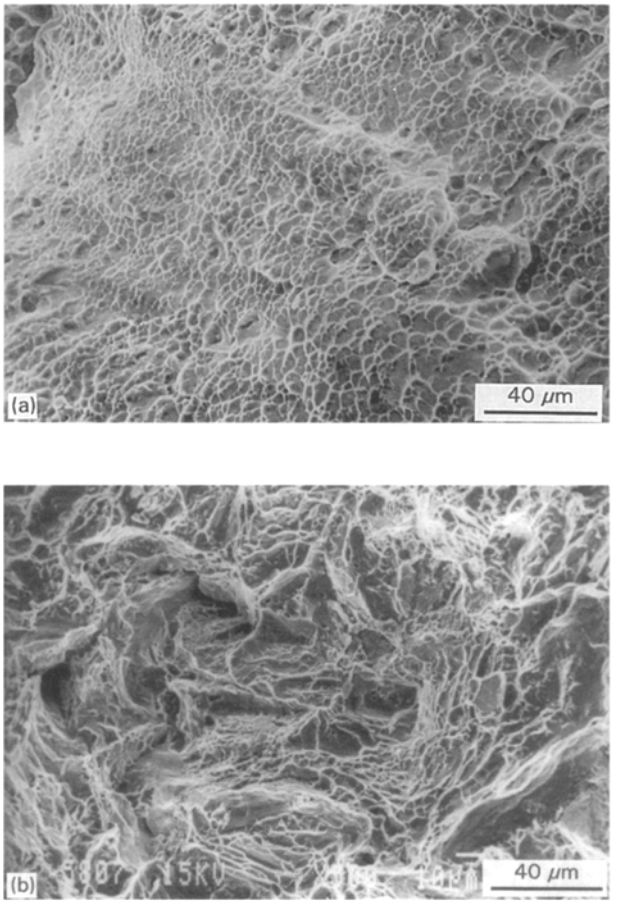

Figure 10 Fractographs in the PWHT conditions: (a) subtransus PWHT and (b) supertransus PWHT.

TABLE VI Data on fusion zone grain widths

Designation of the specimen	Fusion zone grain width (mm)
αβ-120-1	0.158
αβ-200-1	0.077
αβ-260-2	0.075
β-200-1	0.194
β-260-2	0.223

Intergranular fracture in β-base welds is due to the wider fusion zone grains. For the same reason the ductility of β-welds is lower compared to α + β-base welds. The observed higher UTS of smaller grain size α + β-base welds compared to the β-welds containing wider fusion zone grains is in conformity with similar trends reported in the literature [12]. Reduction in strength and improvements in ductility observed during the course of PWHT in the subtransus (α + β-P960-1-AC) and supertransus regions (α + β-P1030-1/4-FC) is due to the decomposition of α′-phase to α + β-phase and coarsening of α-phase [1, 2, 13, 14]. The lowest strength obtained after supertransus PWHT can be attributed to strain localization effects of continuous grain boundary α-phase coupled with thick transgranular α-phase. The improvement in ductility after PWHT is supported by the predominantly ductile transgranular fracture observed (Fig. 10).

5. Conclusions

Electron beam welding studies on an α + β-Ti alloy have shown the following important trends:

(a) High heat input in single-pass welds resulted in reduced strength and ductility due to strain localization effects between grain boundary alpha and transgranular microstructures as well as between primary and secondary martensites. Intergranular and faceted fracture was observed when heat input was high. Two-pass welds exhibited low ductility for the same reason.

(b) Welds of β-base metal exhibited lower strength and ductility compared to α + β-base metal welds, possibly due to the wider fusion zone grains of β-base welds. For this reason intergranular fracture was observed in β-base welds irrespective of the amount of heat input.

(c) Post-weld heat treatments in the subtransus and supertransus regions resulted in reduced strength and improved ductility. The supertransus treatment gave the lowest strength.

Acknowledgements

The authors are thankful to the Director, Defence Metallurgical Research Laboratory, Hyderabad for the permission to publish this work. Help received from the Gas Turbine Research Establishment, Bangalore in electron beam welding is duly acknowledged.

References

1. W. A. BAESLACK III and C. M. BANAS, *Weld. J.* **60** (1981) 121s.

2. M. A. GREENFIELD and D. S. DUVALL, *ibid.* **54** (1975) 73s.
3. R. P. SIMPSON, *ibid.* **56** (1977) 67s.
4. W. A. BAESLACK III and D. W. BECKER, *Metall. Trans. A* **11A** (1979) 1803.
5. Y. MAHAJAN and W. A. BAESLACK III, *Scripta Metall.* **13** (1979) 77.
6. W. A. BAESLACK III and Y. MAHAJAN, *ibid.* **13** (1979) 959.
7. T. V. VIJAYARAGHAVAN and H. MARGOLIN, *Metall. Trans.* **19A** (1988) 591.
8. M. A. GREENFIELD and H. MARGOLIN, *ibid.* **3** (1972) 2649.
9. H. MARGOLIN and Y. MAHAJAN, *ibid.* **9A** (1978) 781.
10. D. BANERJEE, D. MUKHERJEE, R. L. SAHA and K. BOSE, *ibid.* **14A** (1983) 413.
11. K. R. NARENDRANNATH and H. MARGOLIN, *ibid.* **19A** (1988) 1163.
12. D. W. BECKER, R. W. MESSLER Jr. and W. A. BAESLACK III, in Titanium '80 Science and Technology, Proceedings of the Conference, Kyoto, Japan, May 19–22, Eds H. Kimura and O. Izumi, TMS AIME. **1** (1980) p. 255.
13. W. A. BAESLACK III and A. W. MULLINS, *Metall. Trans.* **15A** (1984) 1949.
14. W. A. BAESLACK III, *Weld. J.* **61** (1982) 197S.

Received 22 February
and accepted 1 December 1995